

(f) There are fixed branch cuts in the J plane which do not move with energy. These arise because the centrifugal term $J(J+1)/r^2$ has been modified to $[J(J+1)-e^4]/r^2$. Thus we may not expect these fixed branch cuts for nonrelativistic potential cases as long as the centrifugal term does not get modified.

(g) The Regge poles considered as a function of energy E are analytic at $E=0$ and have two branch cuts running over the real axis, one from $E=+m$ to $E=+\infty$ and another from $E=-\infty$ to $E=-m$. The significance and implications of the latter are not clear.

In conclusion, we wish to mention that some aspects of the Coulomb scattering problem have also been considered by Goldberger and Blankenbecler.⁸

ACKNOWLEDGMENTS

The author is grateful to Professor Geoffrey F. Chew for his encouragement and many discussions. His thanks are also due to other members of the theoretical group for a number of conversations about Regge poles.

⁸ R. Blankenbecler and M. L. Goldberger, Phys. Rev. **126**, 766 (1962).

Negative Meson Absorption in Liquid Hydrogen*†

M. LEON† AND H. A. BETHE

Laboratory of Nuclear Studies, Cornell University, Ithaca, New York

(Received March 5, 1962)

A theoretical study has been made of the atomic processes involved in the absorption of π^- and K^- mesons in liquid hydrogen, with the main purpose of setting an upper limit on the fraction of K mesons that react with the proton from the P state. The principal mode of de-excitation of the mesonic atom, Auger ionization of neighboring hydrogen atoms, was calculated in Born approximation for all the appropriate initial and final values of n . The Stark mixing process discussed by Day, Snow, and Sucher, which allows S -state reaction from high n orbitals, was calculated quantitatively using an impact parameter method and including the effect of the S -state energy shift. In agreement with Day *et al.*, it was found that practically all of the K^- mesons react from the S state; the actual fraction of P -state reactions is less than 1%. In addition, the calculated cascade time for π^- in liquid hydrogen is compatible with the experimental value.

1. INTRODUCTION

OF importance to the analysis of low-energy \bar{K} -nucleon scattering data is the answer to the question: From what orbital angular momentum states do K^- mesons absorbed in liquid hydrogen react with the protons? In this paper we attempt to place onto a more quantitative footing the conclusion of Day, Snow, and Sucher¹ that the reaction is overwhelmingly from the S state.

Until recently, the final word on the subject of negative meson absorption in hydrogen was that of Wightman.² Wightman was particularly concerned with the π^- , and with demonstrating that π^- decay could not

compete with the moderation, atomic capture, and de-excitation into low atomic orbitals. There is no question of nuclear reaction from the P state simply because the rate for capture is demonstrably much smaller than the nP to $1S$ radiation rate.³ For K^- , in contrast, this is not the case; in fact, the rather meager data indicate that these two rates might be comparable.⁴

The development that has stimulated interest in this problem is the observation of Day *et al.*¹ that the electric fields of neighboring hydrogen atoms cause the K -mesonic atom to make transitions among the degenerate states of principal quantum number n . Since the mesonic atom is neutral, rather small, and has no electrons of its own, it can pass freely into the hydrogen-atom electron cloud where it feels the field from the proton. The resulting "Stark effect" makes the strong S -state absorption effective even for orbital angular momenta $l > 0$. Day *et al.* concluded that this effect suffices to ensure K^- absorption (i.e., inelastic reaction with the proton) at high n via the S state, before the atom can de-excite to low n where P -state capture might be important. Further, Russell and Shaw⁵ pointed out

* Based in part on a thesis submitted by one of us (M.L.) to the Faculty of the Graduate School of Cornell University in candidacy for the degree of Doctor of Philosophy.

† This work was supported in part by the joint contract of the Office of Naval Research and the U. S. Atomic Energy Commission.

‡ Now at the Department of Mathematical Physics, University of Birmingham, Edgbaston, Birmingham, England. Much of this research was performed while this author was a National Science Foundation Cooperative Graduate Fellow.

¹ T. B. Day, G. A. Snow, and J. Sucher, Phys. Rev. Letters **3**, 61 (1959); and Phys. Rev. **118**, 864 (1960); also G. A. Snow, *Proceedings of the 1960 Annual International Conference on High-Energy Physics at Rochester* (Interscience Publishers, New York, 1960), p. 407; and T. B. Day, University of Maryland Physics Department Technical Report No. 175, 1960 (unpublished).

² A. S. Wightman, thesis, Princeton University, 1949 (unpublished); and Phys. Rev. **77**, 521 (1950).

³ K. Brueckner, R. Serber, and K. Watson, Phys. Rev. **81**, 575 (1951).

⁴ L. W. Alvarez, University of California Radiation Laboratory Report UCRL-9354, 1960 (unpublished).

⁵ J. E. Russell and G. L. Shaw, Phys. Rev. Letters **4**, 369 (1960).

that the extremely short cascade time $[(1.2_{-0.5}^{+1.2}) \times 10^{-12}$ sec from meson velocity $=0.01c$ to nuclear reaction] for π^- in liquid hydrogen found by Fields *et al.*⁶ requires absorption from relatively high n , and therefore something like the Stark effect mechanism; and that the same mechanism can be expected to operate for K^- capture.

In order to show in detail how the absorption comes about, we have examined both the Stark mixing process and the competing de-excitation processes. In Sec. 2 the mesonic atoms' most important de-excitation mode, Auger ionization of the neighboring hydrogen atoms, is calculated and compared with radiative de-excitation. Section 3 contains calculations of the Stark mixing for degenerate states, while Sec. 4 includes the effect of the strong-interaction, S -state energy shift. In Sec. 5 these rates are used to follow the life history of the π^- and K^- mesonic atoms, and thus to set an upper limit on the amount of K^- P -state absorption. Finally, Sec. 6 contains a brief discussion.

Unless explicitly indicated otherwise, atomic units are used throughout: $m_e = e = a_0 = \alpha c = \hbar = 1$.

2. DE-EXCITATION PROCESSES

A. Initial Steps

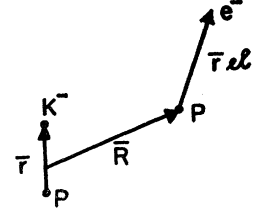
Wightman² estimates the times for a meson to slow down and be captured into a large Bohr orbit, and for the mesonic atom then to be de-excited down to $n \approx \sqrt{M_K}$ (M_K = reduced mass of the mesonic atom) so that the Bohr radius $a_n \approx 1$, by the chemical process $\pi^- H^+ + H_2 \rightarrow \pi^- H_3^+ \rightarrow \pi^- H^+ + H + H$ (and the same thing with K^- instead of π^-). Day⁷ has redone the arithmetic using Wightman's formulas in order to get more accurate numbers. Day's results are:

$$\begin{aligned} \tau \text{ (meson velocity} = 0.05c \text{ to molecular capture)} \\ \approx 3.7 \times 10^{-12} \text{ sec, for } \pi^-, \\ \approx 12 \times 10^{-12} \text{ sec, for } K^-, \end{aligned}$$

$$\begin{aligned} \tau \text{ (meson velocity} = 0.01c \text{ to molecular capture)} \\ \approx 1.2 \times 10^{-12} \text{ sec, for } \pi^-. \end{aligned}$$

The mesonic atom loses $\gtrsim 4.7$ eV in these molecular reactions, and is expected to come out with about one eV in kinetic energy and therefore to have a velocity of about 10^6 cm sec⁻¹. Below $n \approx \sqrt{M_K}$, the

FIG. 1. Coordinate system for Auger cross-section calculation.



chemical process becomes less important; we estimate $\sigma_{chem} \approx \frac{1}{2} \pi a_n^2$.

B. Auger De-excitation

The Auger de-excitation mechanism begins to become significant at the $n \approx \sqrt{M_K}$ stage. We compute the rates using Born approximation.⁸

The coordinate system is shown in Fig. 1; \mathbf{R} connects the c.m. of the mesonic atom with the proton, so that the total KE (kinetic energy) separates into the KE of each atom plus the KE of relative motion.⁹ The part of the interaction that can cause electronic transitions is given by

$$H = |\mathbf{R} - (1-\epsilon)\mathbf{r} + \mathbf{r}_{el}|^{-1} - |\mathbf{R} + \epsilon\mathbf{r} + \mathbf{r}_{el}|^{-1},$$

where ϵ denotes the ratio of masses: $\epsilon = m_K/(m_K + m_p)$; the difference between the c.m. of the H atom and its proton position is neglected. Then using plane waves for the relative motion gives the matrix element

$$H_{if} = (4\pi/q^2) \langle e^{i(1-\epsilon)\mathbf{q} \cdot \mathbf{r}} - e^{-i\epsilon\mathbf{q} \cdot \mathbf{r}} \rangle_{K^-p} \langle e^{-i\mathbf{q} \cdot \mathbf{r}_{el}} \rangle_H,$$

with $\mathbf{q} = \mathbf{k}_i - \mathbf{k}_f$; \mathbf{k}_i and \mathbf{k}_f are the initial and final relative momenta of the atoms. The subscripts K^-p and H indicate the mesonic and hydrogen atoms, respectively.

The Born approximation cross section for ionization is

$$\begin{aligned} \sigma_{if} = \frac{2\pi k_f M_A}{v_i (2\pi)^3} (4\pi)^2 \\ \times \int |\langle \rangle_{K^-p}|^2 |\langle \rangle_H|^2 \frac{k^2}{q^4} dk d\Omega_k d\Omega_{k_f}, \quad (1) \end{aligned}$$

k being the outgoing electron momentum and M_A the reduced mass of the two atoms. Except for the mesonic atom factor $|\langle \rangle_{K^-p}|^2 M_A^2$, this is identical to the Born cross section for ionization of hydrogen by a fast electron, and we can immediately use the result¹⁰

$$\int |\langle \rangle_H|^2 d\Omega_k = 2^8 \frac{q^2 [q^2 + \frac{1}{3}(1+k^2)] \exp[-(2/k) \tan^{-1}(2k/(q^2 - k^2 + 1))]}{k [(q+k)^2 + 1]^3 [(q-k)^2 + 1]^3 [1 - \exp(-2\pi/k)]}. \quad (2)$$

Conservation of energy requires

$$k^2 = 2\Delta E + (k_i^2 - k_f^2)/M_A,$$

and $\Delta E = \Delta E_{K^-p} - \delta_H$, where ΔE_{K^-p} is the energy loss

⁶ T. H. Fields, G. B. Yodh, M. Derrick, and J. G. Fetkovich, Phys. Rev. Letters **5**, 69 (1960).

⁷ T. B. Day, reference 1, Fig. 2 and p. 4.

of the mesonic atom and δ_H is the ionization energy. Then

$$k dk d\Omega_{k_f} = d^3q/k_f M_A. \quad (3)$$

⁸ J. E. Russell and G. L. Shaw, reference 5, have already given the results of what is evidently a similar calculation for a few π -mesonic atom transitions, but no details of the calculation are included. By direct comparison, their cross section values are in

TABLE I. Auger rates for π meson (in units of 10^{10} sec^{-1}). The quantities in parentheses are for molecular dissociation. The transitions indicated by \dots as well as those where quantities in parentheses are given, are energetically impossible. Initial n is at left, final n at top.

	1	2	3	4	5	6	7	8	9	10	11	12
2	0.24											
3	0.016	8.3										
4		0.56	66									
5			4.3	290								
6				19	930							
7					60	2300						
8					11	170	8700					
9						29	310	(29)				
10							62	610	(44)			
11							19	120	\dots	\dots		
12								38	210	(90)	\dots	
13								15	68	\dots	\dots	\dots
14									20	114	\dots	\dots
15							1.2	3.9	14	47	\dots	(220)

Because of the large magnitude of M_A (i.e., because the mesonic atom velocity is negligible compared to the electron velocity), we can put

$$k = (2\Delta E)^{\frac{1}{2}} \quad (4)$$

independent of \mathbf{q} . This independence of \mathbf{q} and k facilitates the integration over d^3q .

To evaluate the meson factor $\langle \rangle_{K^-p}$, we take advantage of the small size of the mesonic atom by expanding the exponentials and retaining only the

dipole term.¹¹ Averaging over m and initial l and summing over final l , we have in terms of the average (hydrogen) radial matrix elements¹²

$$|\langle \rangle_{K^-p}|^2 \approx q^2 M_K^{-2} \frac{1}{3} (R_{n'n})^2. \quad (5)$$

Using Eqs. (2), (3), and (5) in (1) gives for the average Auger cross section

$$\sigma_{if} \approx \frac{16\pi}{v_i M_K^2} \frac{1}{3} (R_{n'n})^2 I(k), \quad (6)$$

where

$$I(k) = \int_0^{q_{\max}} q^2 \frac{2^8 [q^2 + \frac{1}{3}(1+k^2)] \exp[-(2/k) \tan^{-1}(2k/(q^2-k^2+1))]}{[(q+k)^2+1]^3 [(q-k)^2+1]^3 [1-\exp(-2\pi/k)]} dq.$$

$I(k)$ can be evaluated analytically only in the limit: $I(k) \rightarrow k^{-1}$ as $k \rightarrow \infty$; but by numerical integration we find that, to within a few percent,

$$I(k) \approx (k^2 + 1.39)^{-\frac{1}{2}}. \quad (7)$$

Hence, we have for the average rate of Auger de-excitation

$$\Gamma_{if} = N v_i \sigma_{if} \approx 4.3 \times 10^{15} \text{ sec}^{-1} \times (R_{n'n})^2 M_K^{-2} (2\Delta E + 1.39)^{-\frac{1}{2}}, \quad (8)$$

with N = density of hydrogen atoms $\approx 4.3 \times 10^{22} \text{ cm}^{-3}$.

Furthermore, since the rate for discrete excitation of

the H atom goes over smoothly into the continuum case as $n \rightarrow \infty$, we can use Eq. (8) even for $k^2 < 0$. We will switch from this average rate to the explicit formula only for $n=2$, this value being chosen only because $n=3$ corresponds to $n^{-3} \approx 1 \text{ eV} \approx$ mesonic atom KE. Thus Eq. (8) holds for $k^2 \gtrsim -1/9$.

The resulting rates for a wide range of initial and final n for π -mesonic and for K -mesonic atoms are presented in Tables I and II. In contrast to radiation, the Auger process favors transitions with as little change in n as is consistent with supplying the hydrogen ionization energy. In addition, it will be noted that for the largest

agreement with ours, below, but their rates are smaller because they use a smaller value of liquid hydrogen density. The earlier calculation of Wightman (thesis) contains some errors.

⁹ It must be stated that throughout this work we treat the liquid as if it were made up of hydrogen atoms rather than molecules, except for replacing the atomic ionization energy (13.6 eV) by the molecular value (15.2 eV).

¹⁰ E.g., H. A. Bethe, in *Handbuch der Physik* (Springer-Verlag, Berlin, 1933), 2nd ed., Vol. 24, Part 1; N. F. Mott and H. S. W. Massey, *Theory of Atomic Collisions* (Clarendon Press, Oxford, 1949), 2nd ed., Chap. 11; L. D. Landau and E. M. Lifshitz, *Quantum Mechanics, Nonrelativistic Theory* (Addison-Wesley Publishing Company, Reading, Massachusetts, 1958), p. 120.

¹¹ Since $q \sim 1$, one might think that for the dipole approximation to hold, $n^2 \ll M_K$. However, a look at the exact matrix elements, which can be found in rather unwieldy analytic form (see Landau and Lifshitz, reference 10, Appendix f), indicates that only $q \ll [(n-n')/nn'] M_K$ is necessary. This is always satisfied in the present calculations, since $nn' \sim M_K$ is always accompanied by $(n-n') \sim$ several.

¹² E.g., H. A. Bethe and E. E. Salpeter, *Quantum Mechanics of One- and Two-Electron Atoms* (Academic Press Inc., New York, 1957), p. 254. We have evaluated the $(R_{n'n',l})^2$ numerically using Eq. (63.2) of Bethe and Salpeter, and have taken the weighted average over l ; see M. Leon, thesis, Cornell University, 1962 (unpublished), Appendix, for a table of $(R_{n'n'})^2$ values.

TABLE II. Auger rates for K mesons (in units of 10^{10} sec^{-1}). The quantities in parentheses are for molecular dissociation where ionization is energetically impossible. Initial n is at left, final n at top.

	1	2	3	4	5	6	7	8	9	10	11	12	13	14	15	16	17	18
2	0.021																	
3	0.0014	0.71																
4		0.048	5.8															
5			0.37	25														
6			0.076	1.6	83													
7					4.9	210												
8						13	460											
9							30	930										
10								54	1800									
11								10	100	2900								
12									19	170	(11)							
13										33	275	(15)						
14										10	53	430	(21)					
15										4.2	17	85	...	(27)				
16											6.7	25	120	...	(35)			
17												10	38			
18													17	53	...	(55)	...	
19														22	73
20														11	30	(84)
21															15
22															8.1
23															4.7	11

few n_i for which $\Delta n=1$ is possible, the Auger rates are considerably larger than $Nv\pi a_0^2 \approx 4 \times 10^{12} \text{ sec}^{-1}$. Here we expect that the Born approximation is giving too large an answer, but for our purposes it is enough to know that these transitions are fast, i.e., $\Gamma_{if} \gtrsim 4 \times 10^{12} \text{ sec}^{-1}$.

Indeed, a sufficient condition for the Born approximation here employed is that the transition probability for any particular impact parameter be $\ll 1$. Because transition comes only from interaction with the electron, not with the proton, the probability should level off for impact parameter $\rho \lesssim a_0$ and therefore the main contribution to the cross section is from collision with $\rho \gtrsim a_0$. Then $\sigma < \pi a_0^2$ implies that the probability is never ~ 1 for any ρ and hence the Born approximation is justified.

C. Radiative De-excitation

The radiation rates of the mesonic atoms are related to the hydrogen rates by¹³

$$\Gamma_{\text{rad},if} = M_K (\Gamma_{\text{rad},if})_{\text{H}} = \frac{4}{3} (\Delta E)^3 (R_{n_i}^{n_f})^2 M_K^{-2} \times 1.60 \times 10^{10} \text{ sec}^{-1}. \quad (9)$$

Comparing this with the Auger rates Eq. (8), we conclude that radiation is unimportant for all transitions such that $n_f > 3$; radiation will play a role only if the meson survives down to $n=4$.

3. STARK MIXING OF DEGENERATE STATES

Transitions among the n^2 degenerate states of a given n are induced when the mesonic atom passes near, or

¹³ Bethe and Salpeter, reference 12, Sec. 59, 60, 63, and Appendix.

through, a hydrogen atom and "feels" the H atom electric field. The matrix element for this "Stark mixing" is

$$V_{l-1}^l = \langle n, l-1 | \mathbf{F}_0 \cdot \mathbf{r} | n, l \rangle \sim \frac{e^2}{a_0^2} Z_{\text{eff}} R_{n,l}^{n,l-1} M_K^{-1} = n(n^2 - l^2)^{1/2} M_K^{-1} \times 4 \times 10^{16} \text{ sec}^{-1};$$

where Z_{eff} is an effective nuclear charge of the H atom (≤ 1), \mathbf{F}_0 denotes the H atom (shielded) electric field, \mathbf{r} the mesonic atom coordinate, and $R_{n,l}^{n,l-1}$ the resulting hydrogen-like radial dipole matrix element. Hence there is enough time during the collision ($a_0/v \sim 10^{-14} \text{ sec}$) for the atom to make many transitions back and forth among the states, so that the Born approximation is clearly not applicable. Instead, we use an impact parameter method, treating the mesonic atom as a classical particle moving in a definite and undeflected trajectory; the necessary condition on the relative momentum, $k_A \gg 1$, is here satisfied with $k_A \approx 5$ (mesonic atom $KE \approx 1 \text{ eV}$). The transition probability as a function of impact parameter is found by integrating the Schrödinger equation, taking into account transitions among the degenerate states but ignoring the much less likely transitions to states of different n .

A. Rotating Field Model

In this approximation we have a simplified Schrödinger equation for the internal coordinate of the mesonic atom

$$i \frac{\partial}{\partial t} \psi(t) = H(t) \psi(t),$$

where $H(t)$ includes only the perturbing electric field term. Expanding into an orthonormal set of n^2 functions $u_\alpha(t)$ (all corresponding to the same n),

$$\psi(t) = \sum_\alpha a_\alpha(t) u_\alpha(t),$$

we have

$$i\dot{a}_\beta = \sum_\alpha [\langle u_\beta | H | u_\alpha \rangle - i \langle u_\beta | \partial/\partial t | u_\alpha \rangle] a_\alpha. \quad (10)$$

We take the z axis in the (turning) field direction and the x axis in the plane of collision, and let θ denote the angle between x axis and the direction of motion (so that θ goes from $-\pi/2$ to $\pi/2$ as the collision proceeds). Using the eigenfunctions of L^2 and L_z as our orthonormal set, Eq. (10) becomes

$$i\dot{a}_l^m(t) = \sum_{l', m'} [F \langle u_l^m | z | u_{l'}^{m'} \rangle - i \dot{\theta} \langle u_l^m | \partial/\partial \theta | u_{l'}^{m'} \rangle] a_{l'}^{m'}(t), \quad (11)$$

where

$$F = F_0(R(t)) M_K^{-1} = e^{-2R(t)} [1 + 2R(t) + 2R^2(t)] / R^2(t) M_K \quad (12)$$

gives the field strength from a hydrogen atom in its ground state. The $\dot{\theta}$ term contains the effect of using a turning z axis. z has nonvanishing matrix elements only for $\Delta l = \pm 1$, $\Delta m = 0$; and $\partial/\partial \theta = iL_y$ only for $\Delta l = 0$, $\Delta m = \pm 1$. Employing the well-known formulas,¹³ we write Eq. (11) as

$$\begin{aligned} i\dot{a}_l^m = & \frac{3}{2} F n \left[\left[\frac{(l^2 - m^2)(n^2 - l^2)}{(2l+1)(2l-1)} \right]^{\frac{1}{2}} a_{l-1}^m \right. \\ & + \left[\frac{((l+1)^2 - m^2)(n^2 - (l+1)^2)}{(2l+3)(2l+1)} \right]^{\frac{1}{2}} a_{l+1}^m \Big\} \\ & - \frac{1}{2} i \dot{\theta} \{ [l(l+1) - m(m-1)]^{\frac{1}{2}} a_l^{m-1} \\ & - [l(l+1) - m(m+1)]^{\frac{1}{2}} a_l^{m+1} \}. \quad (13) \end{aligned}$$

This set of simultaneous differential equations was integrated numerically (by digital computer) for the particular case of a π -mesonic atom of 1 eV KE and $n=5$, for several values of impact parameter ρ and initial l, m . The results of these computations enable us to draw two general conclusions: (1) Because mixing of the high- l states takes place at large enough ρ to give large mixing cross sections, Wightman's "doldrums" (i.e., an atom getting stuck in a high- n and high- l state because $\Delta n = 1$ is energetically impossible), in fact, cause no difficulty; and indeed the assumption used throughout of uniform *a priori* distribution among all the states except the S state is a good approximation. (2) For the special case of the total probability of transition to and from the S state, the $\dot{\theta}$ terms of Eqs. (11) and (13) can be dropped, resulting in great simplification. We can call Eqs. (11) and (13) the *rotating field model*; then dropping the $\dot{\theta}$ terms produces the *fixed field model*.

B. Field Fixed Model

Because it neglects the effect of having a turning axis of quantization, the fixed field model is equivalent to assuming that, as soon as the mesonic atom feels the electric field, its angular momentum component m becomes fixed in the field direction. Of course this assumption cannot be correct for large separations and impact parameters; however, these regions do not contribute to the cross section anyway. One might have hoped for two fairly disjoint regions: the "outside" where m remains fixed in space and no transition takes place, and the "inside" transition region where m remains fixed in the field direction. Unfortunately, the rotating field model computations show that this definitely is not the case; transitions in m are quenched only for very small separations ($R \lesssim \frac{1}{2} a_0$). Even so, we pursue the fixed field model because it gives for the S state the same results as the more difficult model. That this should be so is perhaps not surprising, since the S state is not related to any other state by $\Delta l = 0$, $\Delta m = \pm 1$.

The simplification comes about because to lowest order the perturbation $H(t)$ is diagonal in the "Stark representation," i.e., when the wave equation is separated in parabolic rather than spherical coordinates. In this representation, Eq. (11) with the $\dot{\theta}$ term omitted,

$$i\dot{a}_{n_1}^m(t) = E_{n_1}(t) a_{n_1}^m(t),$$

is trivial to integrate

$$a_{n_1}^m(t) = a_{n_1}^m(-\infty) \exp \left[-i \int_{-\infty}^t E_{n_1}(t') dt' \right].$$

Here n_1 is one of the parabolic quantum numbers. Therefore, we have as transition probability between angular momentum states

$$P(l, l') = |\sum_{n_1} \langle l | n_1 \rangle e^{-i\Phi(\rho, n_1)} \langle n_1 | l' \rangle|^2. \quad (14)$$

$\Phi(\rho, n_1)$ is the accumulated phase of each Stark state, computed along a trajectory of impact parameter ρ ; using the familiar result for the Stark splitting,¹⁴

$$\begin{aligned} \Phi(\rho, n_1) &= \int_{-\infty}^{\infty} E_{n_1}(t) dt = \int_{-\infty}^{\infty} \frac{3}{2} F n (n_1 - n_2) dt \\ &= \frac{3}{2} \pi \frac{n(n_1 - n_2)}{v M_K} \frac{\zeta(\rho)}{\rho}, \quad (15) \end{aligned}$$

with

$$\zeta(\rho) = \frac{1}{\pi} \int_{-\pi/2}^{\pi/2} e^{-2\rho \sec \theta} (1 + 2\rho \sec \theta + 2\rho^2 \sec^2 \theta) d\theta. \quad (16)$$

n_1 and n_2 are the parabolic quantum numbers satisfying $n_1 + n_2 + m + 1 = n$; the m index of the expansion coefficients is suppressed. These coefficients $\langle n_1 | l \rangle$ were found (cf. Appendix) and the resulting probability matrices for $m=0$ and $n=5, 10$, and 15 computed as a function of $\Delta\Phi$, the phase difference between adjacent

¹⁴ Bethe and Salpeter, reference 12, Sec. 51.

Stark states. Figure 2 gives the resulting S state "isolation" probabilities $P(0,0)$; after $\Delta\Phi = \pi$ the curves just repeat themselves, i.e., $P(2k\pi \pm \Delta\Phi) = P(\Delta\Phi)$ for any integer k .

We are interested in the situation where the mesonic atoms enter the collision with an approximately uniform distribution in l , except for the absence of atoms with $l=0$; we want to find the probability of a transition to $l=0$, which is given by (considering only the $m=0$ states)

$$\frac{1}{n-1} \sum_{l=1}^{n-1} P(0,l) = \frac{1-P(0,0)}{n-1}.$$

Furthermore, we replace the more legitimate Stark mixing cross section

$$2\pi \int_0^\infty \rho d\rho \left[\frac{1-P(0,0)}{n-1} \right],$$

by the more convenient expression $\pi \rho_s^2 n^{-1}$, n^{-1} being the average over $\Delta\Phi$ of $[1-P(0,0)]/(n-1)$. The remaining task of finding the effective impact parameter ρ_s is facilitated both by the rapid decrease of $P(0,0)$ with increasing $\Delta\Phi$, and by the rapid decrease of $\Delta\Phi$ with increasing ρ . It is found that, when plotted against $n\Delta\Phi$ instead of $\Delta\Phi$, the three curves of Fig. 2 coincide almost exactly; in addition, each curve reaches 0.1 at $n\Delta\Phi = \frac{3}{2}\pi$. This enables us to establish as S -state mixing criterion

$$\Delta\Phi(\rho_s) = 3\pi/2n, \quad (17)$$

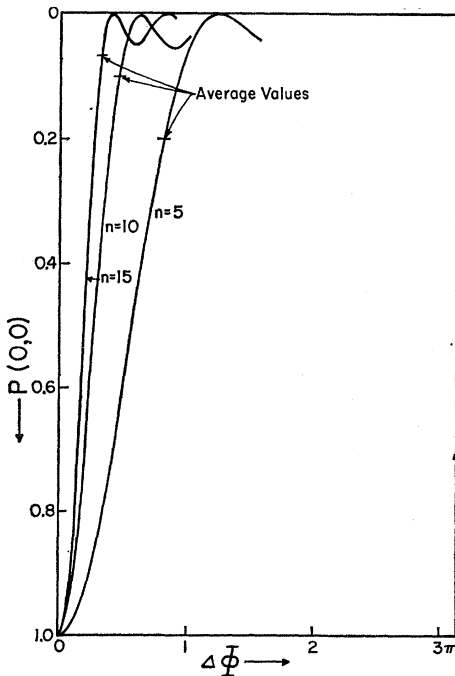


FIG. 2. Isolation probabilities of the S state.

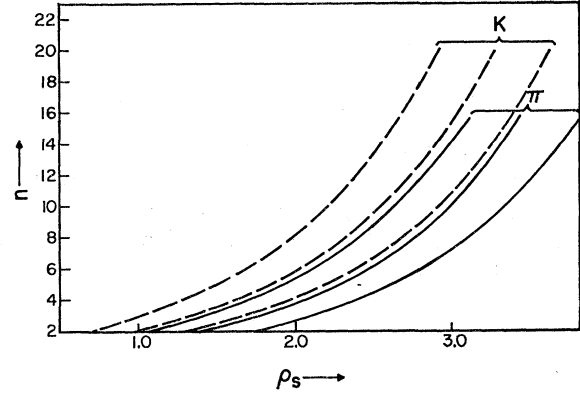


FIG. 3. Effective impact parameter for Stark mixing of S state, for KE of (left to right) 4, 1, $\frac{1}{4}$ eV.

since $\Delta\Phi$ for $P(0,0)=0.1$ is always close to $\Delta\Phi$ for $P(0,0)=n^{-1}$, the more logical choice. Combining Eqs. (15), (16), and (17), ρ_s is the root of the equation

$$\zeta(\rho)/\rho = vM_K/2n^2. \quad (18)$$

The function $\zeta(\rho)$ was computed numerically for a range of ρ ; the resulting ρ_s values are presented as functions of n in Fig. 3. It is notable how insensitive ρ_s is to the mesonic atom KE and likewise to the exact value of $\Delta\Phi$ chosen for the mixing criterion.

Finally, in Fig. 4 we compare the fixed field model and rotating field model results for the S -state isolation

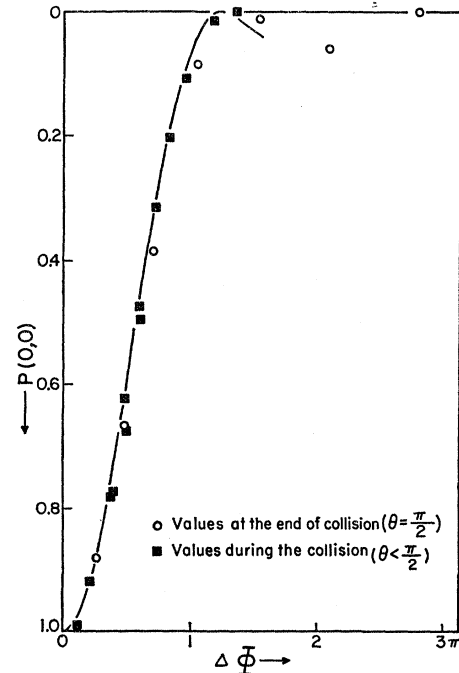


FIG. 4. Comparison of the S -state isolation probability for $n=5$; the points are from the rotating field model, the curve from the fixed field model as in Fig. 2.

probability $P(0,0)$ for $n=5$. As implied above, the agreement is very close.

4. STARK MIXING IN THE PRESENCE OF NUCLEAR INTERACTION

In all the above, we have ignored the process of greatest interest, that is, meson capture by the proton. Since Stark mixing depends upon the degeneracy of the n^2 states, we expect the strong interaction energy shift, which lifts this degeneracy, to play an important role.

A. Nuclear Energy Shifts

The S - and P -state energy shifts are given in terms of the complex meson-proton scattering lengths by¹⁵

$$\begin{aligned}\delta E_S &= -2\pi A_S |\psi(0)|^2 M_K^{-1} = -2A_S M_K^2 n^{-3}, \\ \delta E_P &= -6\pi (A_P/k^2) |\nabla\psi(0)|^2 M_K^{-1} \\ &= -2(A_P/k^2) M_K^4 (n^2 - 1/n^5),\end{aligned}\quad (19)$$

using hydrogenic wave functions for the density factors. As usual, the imaginary part of the energy shift gives the capture rate. As far as interference with Stark mixing is concerned, only the S -state scattering lengths are large enough to matter; below we put $\delta E \equiv \delta E_S$. For π^- ,¹⁶ $A_S \approx (0.11 + i0.0051)$ f, while for K^- we have taken¹⁷ $A_S \approx (1 + i)$ f. In the P state, for π^- the capture is negligible as stated above,¹⁸ while for K^- a reasonable guess is $\text{Im}(A_P/k^2) \approx 0.04$ f³.¹⁹

B. Interference with Stark Mixing

To assess the effect of the interference with mixing, we first determine how strong an electric field is needed for the mixing to overcome the displacement in energy of the S state. To do this, we consider as in the fixed field model the n states with $m=0$, and include δE in the Hamiltonian.²⁰ Diagonalizing this complex Hamiltonian is relatively easy because the electric field perturbation is diagonal in the Stark representation, and because the expansion coefficient $\langle n_1 | l=0 \rangle = n^{-1/2}$ for any n_1 . Thus,

$$i\dot{a}_{n_1} = \sum_{n_1'} \langle n_1 | H_{\text{Stark}} | n_1' \rangle a_{n_1'} + \delta E \langle n_1 | l=0 \rangle \sum_{n_1'} \langle l=0 | n_1' \rangle a_{n_1'}, \quad (20)$$

$$i\dot{a}_{n_1} = E_{n_1} a_{n_1} + (\delta E/n) \sum_{n_1'} a_{n_1'}.$$

If the set (a_{n_1}) is an eigenvector with eigenvalue λ , Eq. (20) gives

$$a_{n_1} = \frac{\delta E}{n(\lambda - E_{n_1})} \sum_{n_1'} a_{n_1'};$$

¹⁵ S. Deser, M. L. Goldberger, K. Bauman, and W. Thirring, *Phys. Rev.* **96**, 774 (1954).

¹⁶ G. Puppi, *Proceedings of the 1958 Annual Conference on High-Energy Physics at CERN* (CERN Scientific Information Service, Geneva, 1958), p. 42.

¹⁷ R. H. Dalitz, *Revs. Modern Phys.* **33**, 471 (1961).

¹⁸ K. Brueckner *et al.*, reference 3, or directly from the P -wave scattering lengths, Puppi, reference 16.

¹⁹ L. W. Alvarez, reference 4. This corresponds to a P -wave absorption cross section of 20 mb at 400 MeV/c (lab.).

²⁰ A similar situation for $n=2$ was treated by Bethe and Salpeter, reference 12, Sec. 67.

summing over n_1 , substituting for E_{n_1} as in Eq. (15), and setting $\gamma \equiv 2i\delta E/3Fn^2$, $\beta \equiv \lambda/3Fn$, we get the remarkably simple eigenvalue equation for β

$$\sum_{j=-\frac{1}{2}(n-1)}^{\frac{1}{2}(n-1)} \frac{1}{j-\beta} = \frac{2}{i\gamma}. \quad (21)$$

For small $|\gamma|$, i.e., Stark splitting \gg energy shift, the β eigenvalues are close to the real values $-\frac{1}{2}(n-1)$, $-\frac{1}{2}(n-1)+1$, \dots , $\frac{1}{2}(n-1)$, so that the energy eigenvalues are only slightly perturbed from their Stark values. Thus

$$\beta \approx j_0 - (i/2)\gamma, \quad (22)$$

$$\lambda \approx 3Fnj_0 + \delta En^{-1}, \quad j_0 = -(n-1)/2, \dots, (n-1)/2,$$

with the result that each eigenstate has the expected fraction n^{-1} of the S -state capture.

At the other extreme of large $|\gamma|$, one β eigenvalue is large in absolute magnitude,

$$\beta_S \approx -(i/2)n\gamma, \quad \lambda_S \approx \delta E;$$

this is in fact just the slightly perturbed S state. The eigenvalues of the remaining $n-1$ states again lie close to the real axis between the original n Stark eigenvalues; the corresponding eigenstates are combinations of the $n-1$ $l>0$ states. So here we see how the S state is separated from the others by its strong interaction with the proton. Furthermore, for this perturbed S state

$$\beta_S \approx -(i/2)n\gamma[1 - (n^2 - 1)/(3n^2\gamma^2)];$$

then since $\sum \beta_i = -(i/2)n\gamma$, we have for the *average* energy shift of the " $l>0$ " eigenstates

$$\begin{aligned}\langle \beta_{l>0} \rangle_{\text{av}} &\approx i(n+1/6n\gamma), \\ \langle \lambda_{l>0} \rangle_{\text{av}} &\approx i(n+1/6n)(3Fn)^2/\delta E.\end{aligned}\quad (23)$$

Thus the S -state mixing is very small at this extreme of $|\gamma| \gg 1$; a sufficiently strong electric field is needed to bring about Stark mixing and capture.

Besides these two extremes, we are interested in the region $|\gamma| \sim 1$. First we consider pure imaginary δE , so



FIG. 5. Complex β eigenvalues for $n=7$. Successive values of $\gamma=0, 0.2, 0.4, 0.6, 0.7, 0.8, 1.0, 1.3, 1.8, 4.0$.

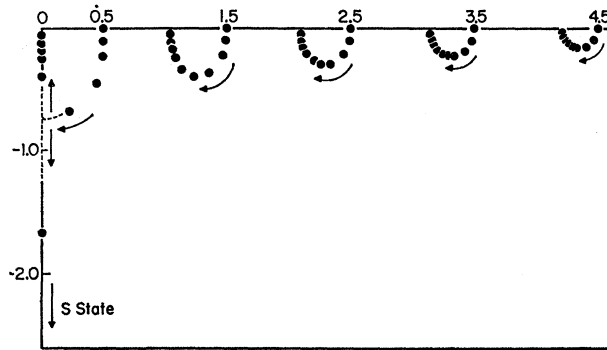


FIG. 6. Complex β eigenvalues for $n=10$. Successive values of $\gamma=0, 0.2, 0.4, 0.6, 0.7, 0.8, 1.0, 1.3, 1.8, 4.0$.

that γ is real. We have used a digital computer to find the roots of Eq. (21) as a function of γ for several values of n . Results for $n=7$ and 10 are presented in Figs. 5 and 6. The half-plane corresponding to positive real parts is shown; the negative half-plane is just its mirror image. The arrows indicate the direction of migration of the eigenvalues, starting from the Stark state values, as γ is increased. The increasing isolation of the perturbed S state is apparent.

For n odd, the S state arises from the unshifted Stark state (Fig. 5). For n even, on the other hand, there is no unshifted Stark state, and because of this we see a rather interesting effect (Fig. 6). As γ increases, the eigenvalues of the two states of smallest Stark shift (those starting at $\beta = \pm 0.5$) move down and toward the imaginary axis, meeting it and each other when $\gamma \sim 1$ ($\gamma = 0.72$ for $n=10$). As γ is increased further, linear combinations of these states separate, one moving up the imaginary axis to form another " $l>0$ " state, the other moving down to form the S state.²¹ This phenomenon gives rise to the possibility of an adiabatic transition from the unshifted " $l>0$ " state to the S state.

The behavior of the β eigenvalues as a function of γ is very much the same for different values of n . This is demonstrated in Fig. 7, where we have plotted the ratio \mathcal{R} of the average capture rate for the " $l>0$ " states to the strong-field value. Points for the extreme examples $n=4$ and $n=15$ fall very close together, and indeed very close to the curve representing the large $|\gamma|$ expansion. Most of the transition from S and " $l>0$ " states to Stark states takes place in the region $0.7 < \gamma < 1.2$, and the rise would appear even steeper if considered as a function of distance from the perturbing hydrogen atom.

For the more relevant case of $\text{Re} \delta E \neq 0$, the eigenvalues are no longer symmetric with respect to the imaginary axis. Furthermore, it need not be the unshifted Stark state (or a combination of the two least shifted states) that becomes the S state as $|\gamma|$ is made

²¹ When high-order perturbations are taken into account, this intersection will become a near miss; the "no crossing" theorem still holds.

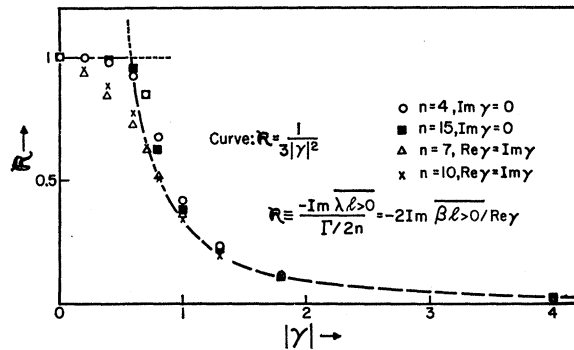


FIG. 7. Degree of Stark mixing of the " $l>0$ " states.

large; this depends on the phase of δE . For $\text{Re} \delta E = \text{Im} \delta E$ we find in fact that it is the most (negatively) shifted state that becomes the S state. However, even for this δE , the behavior of \mathcal{R} is quite close to what it is for $\text{Re} \delta E = 0$, as Fig. 7 shows for $n=7$ and $n=10$.

We now have a second condition necessary for Stark mixing; besides sufficient accumulated phase difference between Stark states, the electric field must be strong enough to overcome the energy shift of the S state. Curves of the separations needed to achieve (for the $\text{Re} \delta E = 0$ case again) $\mathcal{R} = 0.9$ ($\gamma = 0.66$) and $\mathcal{R} = 0.5$ ($\gamma = 0.9$) are given in Fig. 8; the curves from the phase difference condition have been included for comparison. Over the entire n range of interest, the "strong field" condition is the more restrictive for K mesons, while for π mesons it is the phase difference condition that prevails. This circumstance simplifies the remaining task of finding the effective S -state absorption rates.

In what follows it is sufficient approximation to use for $\mathcal{R}(\gamma)$ the formula:

$$\mathcal{R}(\gamma) = 1, \quad |\gamma| < 0.58, \quad R < R_0 \\ = \frac{1}{3} |\gamma|^{-2}, \quad |\gamma| > 0.58, \quad R > R_0. \quad (24)$$

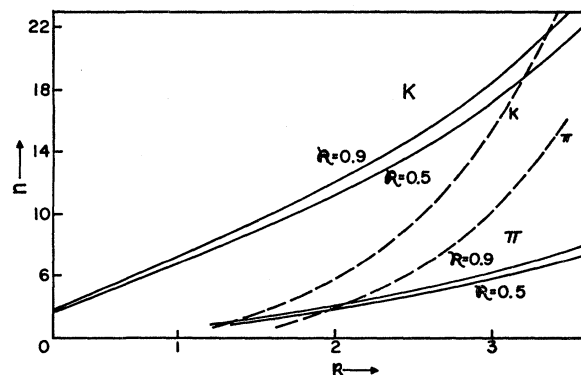


FIG. 8. Approach distance needed to mix the shifted S state (solid curves). For comparison, the 1 eV curves for ρ_S (Fig. 3) are included (broken curves).

C. Effective Nuclear Absorption Rates

For π 's the S -state capture rate $\Gamma_c(n, S) = \Gamma_S n^{-3}$ is a modest $1.1 \times 10^{15} \text{ sec}^{-1} n^{-3}$, so that there is not time for significant depletion of the S state inside the strong field region. But for $n \lesssim 6$ the time *between* Stark collisions is long enough to allow some depletion, and therefore the effective absorption rate $\Gamma_{\text{eff}}(n, S)$ is reduced from the uniform distribution value $\Gamma_S n^{-5}$ to

$$\Gamma_{\text{eff}}(n, S) = \Gamma_{\text{St}}(n) n^{-2} \{1 - \exp[-\Gamma_S / n^3 \Gamma_{\text{St}}(n)]\}. \quad (25)$$

The rate for Stark mixing is given by

$$\Gamma_{\text{St}}(n) = N v \pi \rho_s^2(n) \approx 4.9 \times 10^{12} \text{ sec}^{-1} \rho_s^2(n). \quad (26)$$

The resulting effective absorption rates are given in Table III.

In contrast, the capture rate for K mesons $\approx 1.3 \times 10^{18} \text{ sec}^{-1} n^{-3}$, is so large that depletion is complete between collisions, and is even important *during* the collision. This last fact introduces considerable complication, because it requires us to know how much each of $n^2 - 1$ states is mixed with the S state. The results of the rotating field model (*cf.* Sec. 2) show that $m \neq 0$ states *are* mixed with the S state, and we could find $\Gamma_{\text{eff}}(n, S)$ unambiguously by performing similar computations with an absorption term included. Such a procedure would, however, entail a rather large amount of computation, whereas a much more approximate answer will suffice for our goal of setting an upper limit to the P -state capture.

Such an upper limit requires a lower limit for $\Gamma_{\text{eff}}(n, S)$; this we obtain by assuming that only the n states with $m=0$ are mixed during the collision, and then using $\mathcal{R}(R)$ as a measure of the strength of the mixing. Thus we set

$$\Gamma_{\text{eff}}(n, S) = \frac{vN}{n} \int_0^\infty 2\pi \rho d\rho \times \left\{ 1 - [1 - \mathcal{R}(\rho) n^{-1}] \exp \left[-\frac{\Gamma_S}{v n^4} \int \mathcal{R}(R) dX \right] \right\}; \quad (27)$$

n^{-1} is the probability that an atom have $m=0$, while the $\mathcal{R}(\rho) n^{-1}$ term comes from the atom being left in the S state after the collision; $\mathcal{R}(\rho)$ has been inserted because we know that the cross section cuts off for large ρ . Even

TABLE III. Effective absorption rate for pions. For $n > 6$, depletion is negligible so that $\Gamma_{\text{eff}}(n, S) = \Gamma_S n^{-5}$. Rates are in units of 10^{12} sec^{-1} .

n	$\Gamma_{\text{St}}(n)$	$\Gamma_S n^{-5}$	$\Gamma_{\text{eff}}(n, S)$
3	8.3	4.5	0.92
4	19	1.1	0.70
5	25	0.35	0.30
6	30	0.14	0.13
8	37	0.034	0.034

this Eq. (27) we want to simplify, by considering large n and small n separately.

For large n ($\gtrsim 10$), almost all of the contribution comes from the region where $\mathcal{R}(R) \approx 1$; i.e., $R < R_0$. Therefore we neglect the "tail" where $\mathcal{R}(R) \approx \frac{1}{3} |\gamma|^{-2}$. Then

$$\begin{aligned} \Gamma_{\text{eff}}(n, S) &= \frac{vN}{n} \int_0^{R_0} 2\pi \rho d\rho \\ &\times \{1 - (1 - n^{-1}) \exp[-2\Gamma_S (R_0^2 - \rho^2)^{1/2} v^{-1} n^{-4}]\} \\ &= vN n^{-1} \pi R_0^2 G(\alpha), \end{aligned} \quad (28)$$

with

$$G(\alpha) = \{1 - 2\alpha^{-2} (1 - n^{-1}) [1 - (1 + \alpha)e^{-\alpha}]\}$$

and

$$\alpha = 2\Gamma_S R_0 v^{-1} n^{-4}.$$

For small n ($\lesssim 8$), on the other hand, the "tail" is very important and the absorption falls off gradually with distance. As an approximation, we use the same Eq. (28), but with ρ_1 replacing R_0 ; ρ_1 being the impact parameter for which

$$\Gamma_S v^{-1} n^{-4} \int_{-\infty}^{\infty} \frac{1}{3} |\gamma(R)|^{-2} dX = 1.$$

The $G(\alpha)$ factor is included to ensure smooth joining with the large- n region, but is here unimportant. The required integral

$$\begin{aligned} &\int_{-\infty}^{\infty} \frac{1}{3} |\gamma|^{-2} dX \\ &\sim \rho^{-3} \int_{-\pi/2}^{\pi/2} e^{-4\rho \sec\theta} (1 + 2\rho \sec\theta + 2\rho^2 \sec^2\theta)^2 \sec^{-2}\theta d\theta, \end{aligned}$$

was obtained for a range of ρ by numerical integration.

The resulting rates are given in Table IV. It will be noted that we have been quite conservative for each n range, in keeping with the desire for a lower limit on $\Gamma_{\text{eff}}(n, S)$.

TABLE IV. Effective absorption rate for K mesons. Rates are in units of 10^{12} sec^{-1} .

n	R_0	ρ_1	$\Gamma_S n^{-5}$	$\Gamma_{\text{eff}}(n, S)$
3	0.2	0.31	5400	0.14
4	0.27	0.53	1300	0.30
5	0.5	0.83	420	0.57
6	0.7	0.95	170	0.62
8	1.2	1.3	40	0.84
10	1.6	1.6	13	0.79
12	2.0	(< R_0)	5.2	0.81
16	2.7	(< R_0)	1.2	0.67
18	3.0	(< R_0)	0.69	0.39
20	3.2	(< R_0)	0.41	0.22
23	3.4	(< R_0)	0.20	0.093

5. LIFE HISTORY OF THE MESONIC ATOM

We now have enough information to construct a detailed history of the system, from high n to capture. For the sake of definiteness, we start off with a π -mesonic atom of $n=15$ distributed uniformly in probability among the n^2 states.²² Table V shows the relevant rates and resulting de-excitation and capture sequence. Because of the branching in de-excitation, only a fraction of the mesons go through any particular high n (>7) state, as shown in the table by the "fraction arriving" in these states. Practically all mesons go through the states $n \leq 7$ but at $n=5$, capture begins to be important and decreases the number arriving at $n \leq 4$. We have retained the rather oversize Auger rates for $n=8, 7$, and 6 ; as long as these are large, they have only slight influence on either the lifetime or the distribution of capture. Most of the capture takes place in the $n=4$ and 3 states, only a small fraction making it down to the $2P$ state; and radiation plays practically no part.

The observed π^- cascade time of Fields *et al.*⁶ is $\tau = (1.2_{-0.5}^{+1.2}) \times 10^{-12}$ sec. From this must be subtracted the time required to reach $n=15$, which Day⁷ estimates to be 1.2 (10^{-12} sec will be understood for this section), so there is not much time left for $n=15$ to capture. Corresponding to Table V we find $\tau_{15-0} = 2.3$. The initial stage, $n=15$ to 7 , is rapid: $\tau_{15-7} = 0.8$; this number is affected by our estimate of σ_{chem} for the high n , as well as the mesonic atom velocity. If $\Gamma_{\text{chem}} = Nv\sigma_{\text{chem}}$ is left out altogether $\tau_{15-7} = 1.7$; so that Γ_{chem} evidently belongs and is perhaps underestimated.

We get more significant information from the $n=7$ to

TABLE V. Capture schedule for pions. Rates are in units of 10^{12} sec^{-1} .

n	$\Gamma_{\text{chem}} + \Gamma_{\text{Auger}}$	$\Gamma_{\text{eff}}(n, S)$	$\Gamma_{\text{rad}}(n)$	Fraction	
				Arriving	Captured— S
15	2.9	10^{-3}		1.00	
12	3.4			0.77	
10	7.2	0.011		0.36	
9	3.7	0.019		0.55	0.003
8	89	0.034		0.46	
7	24	0.065		0.94	0.003
6	9.5	0.13		0.96	0.013
5	2.9	0.30		0.95	0.09
4	0.67	0.70	0.007	0.87	0.44
3	0.083	0.92	0.023	0.43	0.39
2	0.0024	~ 1.5	0.15	0.042	0.04

capture stage. Here we have $\tau_{7-0} = 1.5$. If there were no Stark mixing this time would be $\tau_{7-0} = 16$; here we have strong evidence for the presence of the Stark mixing effect,²³ and can be sure that we have not overestimated it.

The corresponding capture schedule for K mesons, starting from $n=23$, including the effect of radiation and branching in feeding the low n states, is given in Table VI. Again the population of high n states ($n > 10$) is depressed by branching while nearly all mesons go through the states $n \leq 10$. However, because of the much greater cross section for nuclear capture, more than half the captures (all from S states) take place for $n > 10$, and less than 4% survive to $n=4$.

To determine the fraction captured in P states we use the experimental estimate¹⁹ of the P -state absorption $\text{Im}(A_{Pk^{-2}}) = 0.04 \text{ f}^3$, and find for the nuclear

TABLE VI. Capture schedule for K mesons. Rates are in units of 10^{12} sec^{-1} .

n	$\Gamma_{\text{chem}} + \Gamma_{\text{Auger}}$	$\Gamma_{\text{eff}}(n, S)$	$\Gamma_{\text{rad}}(n)$	$\Gamma_{\text{eff}}(n, P)$	Arriving	Fraction	
						Captured— S	Captured— P
23	1.9	0.093			1.00	0.05	
20	1.3	0.22			0.88	0.13	
18	1.3	0.39			0.49	0.11	
16	1.9	0.67			0.21	0.05	
15	1.3	0.70			0.22	0.07	
14	5.1	0.74			0.28	0.04	
13	3.1	0.77			0.16	0.03	
12	1.9	0.81			0.33	0.10	
11	30	0.80			0.17	0.01	
10	19	0.79			0.38	0.02	
9	9.6	0.82			0.38	0.03	
8	4.7	0.84			0.35	0.07	
7	2.1	0.73			0.29	0.08	
6	0.85	0.64		0.003	0.21	0.10	
5	0.25	0.57		0.007	0.11	0.08	0.001
4	0.058	0.30	0.019	0.02	0.036	0.03	0.002
3	0.0071	0.14	0.062	0.08	0.006	0.003	0.002
			3P: 0.12 3D: 0.041	3P: 0.24			

²² Since we use $\Gamma_{\text{Auger}}(n)$ averaged over l , we are in fact assuming that the distribution remains uniform. The Stark mixing of the $l > 0$ states ensures this condition (see Sec. 2).

²³ J. E. Russell and G. L. Shaw, reference 5 and T. B. Day, reference 1, have used the π data for the K -meson case in just this way.

capture rate from P states

$$\Gamma_{\text{cap}}(n, P) = 7 \times 10^{12} \text{ sec}^{-1} (n^2 - 1) / n^5$$

and

$$\Gamma_{\text{eff}}(n, P) = 3n^{-2} \Gamma_{\text{cap}}(n, P).$$

The results are listed in Table VI, and show that $\Gamma_{\text{eff}}(n, P)$ is negligible compared with $\Gamma_{\text{eff}}(n, S)$ for $n \geq 5$. Only for $n=4$ does P capture begin to have a fighting chance, and by this time very few mesons survive. The resulting total P -state capture is only half a percent. Even this is an upper limit because the S capture is if anything underestimated—at least judging from the observed capture time for the π meson. Even allowing for the uncertainty in the scattering length, we can conclude that the P -state capture is less than 1%. The cascade time (actually an upper limit) is 2.4.

Table VI is the result of a rather detailed calculation, but it will be seen that the same conclusion can be reached without considering every individual transition. That is, we note that from $n=16$ down to $n=5$ the lower limit on the effective S -state capture is roughly constant, $\Gamma_{\text{eff}}(n, S) \approx 0.7 \times 10^{12} \text{ sec}^{-1}$, while the P -state capture remains negligible. Now since the time to go through this range by Auger de-excitation is about 3.3, only approximately $\exp(-0.7 \times 3.3) \approx 0.10$ of the mesons survive down to $n=5$. For $n < 5$ the Auger rate drops off much faster than does the S -capture rate, so that the large ratio of $\Gamma_{\text{eff}}(n, S)$ to $\Gamma_{\text{Auger}}(n)$ for $n=5$ and $n=4$ kills off 90% of these survivors, leaving less than 0.01 for $n=3$ where P -state capture is strong.

6. DISCUSSION

We conclude by discussing briefly the major approximation made in this work, that is, the use of the impact parameter method. The validity of this classical approximation requires that the relative momentum of the atoms satisfy $k_A \gg 1$. Furthermore, conservation of angular momentum requires deflection of the trajectories, which we have here neglected. This neglect is justified as long as $k_A \gg 1$; the effect becomes more important for smaller mesonic atom velocity, and requires that the cross section for Stark mixing vanish in the small velocity limit. Indeed, this is just the objection that Adair²⁴ made to the original paper of Day *et al.*¹ where a velocity of 10^5 cm sec^{-1} was assumed, corresponding to $k_A \approx 0.5$. The velocity of 10^6 cm sec^{-1} used here satisfies the above inequality fairly well with $k_A \approx 5$, so that we expect this angular momentum conservation effect to be unimportant and the impact parameter method to be reliable.

Clearly, it would be desirable to evaluate the Stark mixing for low velocities by a wave treatment of the relative atomic coordinates, and then to see how the cross section values join the impact parameter method

answers as the velocity is increased. However, even for a low- n mesonic atom and including only the first few partial waves of the relative coordinates, we are left with many simultaneous coupled radial wave equations to solve, and no useful approximations; a prohibitive amount of numerical analysis seems unavoidable.

Throughout this work, we have assumed a mesonic atom KE of 1 eV, because this is about what is expected from the molecular dissociation process. Actually, of course, there is a distribution of energies and velocities, and the mesonic atom in its travels will be slowed down somewhat by elastic scattering. Because of the shortness of the times involved, and also because the scattering is from hydrogen molecules, not atoms, the moderation is not significant; and since the relevant rates do not vary drastically with the velocity, the use of a single average velocity is a good approximation.

Furthermore, there is at least one process which will increase the velocity, namely inelastic Stark collisions. We have treated the Stark effect as splitting states of given principal quantum number n into Stark states of different n_1 . However, if the mesonic atom penetrates deeply into the H atom, the energy curves of states of different n may cross: then the possibility exists that the mesonic atom changes its n and its kinetic energy changes accordingly. Now the kinetic energy is so small that it is usually impossible for it to decrease (or at least very improbable because of the factor $v_{\text{fin.}}/v_{\text{init.}}$ in the cross section) so that these processes generally lead to an increase of kinetic energy and a decrease of n , usually by one unit. In other words this is another mechanism for de-excitation of the mesonic atom. Since we believe that this process is quite likely, we expect that the KE may often be of the order of the energy difference between states of successive n which is a few eV. These inelastic processes are of course another mechanism for transfer of angular momentum from the internal motion of the mesonic atom to the translation.

Finally, we emphasize that the cascade time for the K^- is an upper limit, but not so for the π^- . We estimate

$$\pi^-: \tau = (2.3_{-0.7}^{+1.4}) \times 10^{-12} \text{ sec},$$

$$K^-: \tau = (2.4_{-1.3}^{+0.8}) \times 10^{-12} \text{ sec},$$

to go from $n \approx \sqrt{M_K}$ to capture. While there is no striking agreement between the calculated total π^- cascade time of $3.5 \times 10^{-12} \text{ sec}$ and the observed $1.2 \times 10^{-12} \text{ sec}$, the two values are compatible when the theoretical and experimental uncertainties are considered. The fraction of K mesons reacting from P states is certainly less than 1%, and probably less than 0.5%.

APPENDIX. EXPANSION COEFFICIENTS CONNECTING ANGULAR MOMENTUM AND STARK EIGENSTATES

The coefficients relate the wave functions separated in spherical and parabolic coordinates, respectively;

²⁴ R. K. Adair, Phys. Rev. Letters 3, 438 (1959).

that is,

$$u_{n,l,m}(r,\theta,\varphi) = \sum_{n_1=0}^{n-m-1} \langle l | n_1 \rangle u_{n_1,n_2,m}(\xi,\eta,\varphi). \quad (\text{A1})$$

The spherical and parabolic coordinate systems are related by

$$\begin{aligned} \xi &= r(1 + \cos\theta), \\ \eta &= r(1 - \cos\theta), \\ \varphi &= \varphi. \end{aligned} \quad (\text{A2})$$

By inserting the explicit forms of the wave functions in terms of Laguerre polynomials and Legendre functions²⁵ in (A1), substituting (A2) in the right-hand side, taking $\cos\theta=1$, and equating powers of r , we get the

²⁵ H. A. Bethe and E. E. Salpeter, reference 12, Sec. 3 and 6.

following relation:

$$\begin{aligned} (-)^{l+m} & \left[\frac{(l-m)!(n-l-1)!}{(l+m)!(n+l)!} (2l+1) \right]^{\frac{1}{2}} \\ & \times \frac{2^m s!}{[s-(l-m)]!} \binom{n+l}{l+m+1+s} \frac{d^m P_l(1)}{dz^m} \\ & = \sum_{n_1=s}^{n-m-1} \left[\frac{n_1! n_2!}{(n_1+m)!(n_2+m)!} \right]^{\frac{1}{2}} \\ & \times \binom{n_1+m}{s+m} \binom{n_2+m}{m} \langle l | n_1 \rangle. \end{aligned} \quad (\text{A3})$$

That the left-hand side is zero for $s < l-m$, is to be understood. Equation (A3) is used as a recursion relation to derive all of the coefficients $\langle l | n_1 \rangle$.

Meromorphic Property of the S Matrix in the Complex Plane of Angular Momentum

HUNG CHENG

Physics Department, California Institute of Technology, Pasadena, California

(Received February 16, 1962)

A proof is given for the meromorphic nature of the S matrix in the entire complex plane of the angular momentum, under quite general assumptions for the potential. Some properties for the S matrix in the complex angular momentum plane are discussed.

THE S matrix for the Schrödinger equation has been shown by Regge¹ to be meromorphic in the complex plane of the angular momentum ν to the right of the line $\text{Re } \nu = \max(-3/2, -1/2 - c)$, if the potential $V(x) \rightarrow V_0 x^{2c-2}$ as $x \rightarrow 0$. We here propose a method to enable us to establish the meromorphic property of the S matrix for the Schrödinger equation in the whole ν plane.

The Schrödinger equation is

$$[(d^2/dx^2) - \nu(\nu+1)/x^2] \psi(k, \nu, x) = U(x) \psi(k, \nu, x), \quad (1)$$

where

$$U(x) \equiv V(x) - k^2,$$

with the boundary condition

$$\psi(k, \nu, x) \rightarrow x^{\nu+1}, \quad x \rightarrow 0.$$

Regge transformed this differential equation into an integral equation, with its solution obtained from iteration

$$\psi(k, \nu, x) = x^{\nu+1} + \int_0^x \frac{(x^{\nu+1}/y^\nu - y^{\nu+1}/x^\nu)}{(2\nu+1)} U(y) \psi(k, \nu, y) dy.$$

¹ T. Regge, *Nuovo cimento* **14**, 951 (1959), also *Nuovo cimento* **18**, 947 (1960).

The iteration process fails if the integrals in the iteration diverge ($\int_0^x y^a dy$ diverges if $\text{Re } a \leq -1$) and some integrals in every order of the iteration were indeed found to diverge for $\text{Re } \nu \leq \max(-3/2, -1/2 - c)$.

Instead, we define a linear operator K_ν ,

$$K_\nu(x^\nu) \equiv x^{\nu+2}/(\nu+2)(\nu+1); \quad (2)$$

we are guided by the fact that

$$\int_0^x \frac{x^{\nu+1}/y^\nu - y^{\nu+1}/x^\nu}{2\nu+1} y^\nu dy = \frac{x^{\nu+2}}{(\nu+2)(\nu+1)},$$

if the integral does not blow up at the lower limit of integration. Now, $K_\nu(f(x))$ is defined if $f(x)$ is a sum of terms x^ν , or an infinite, absolutely convergent series of terms x^ν . The power ν does not have to be an integer; in fact, it does not even have to be real. As

$$\frac{d^2}{dx^2} K_\nu(x^\nu) = x^\nu + \nu(\nu+1)/x^2 K_\nu(x^\nu); \quad (3)$$

we have, in general, if $K_\nu(f(x))$ exists,

$$\frac{d^2}{dx^2} K_\nu(f(x)) = f(x) + \nu(\nu+1)/x^2 K_\nu(f(x)).$$